

## Novel Tools and Methods

# How Do Spike Collisions Affect Spike Sorting Performance?

 Samuel Garcia,<sup>1,\*</sup> Alessio P. Buccino,<sup>2,\*</sup> and  Pierre Yger<sup>3,\*</sup>

<https://doi.org/10.1523/ENEURO.0105-22.2022>

<sup>1</sup>Centre de Recherche en Neurosciences de Lyon, Centre National de la Recherche Scientifique, Lyon 69500, France, <sup>2</sup>Department of Biosystems Science and Engineering, ETH Zurich 8092, Switzerland, and <sup>3</sup>Institut de la Vision, Sorbonne Université, Institut National de la Santé et de la Recherche Médicale, Paris 75012, France

## Abstract

Recently, a new generation of devices have been developed to record neural activity simultaneously from hundreds of electrodes with a very high spatial density, both for *in vitro* and *in vivo* applications. While these advances enable to record from many more cells, they also challenge the already complicated process of spike sorting (i.e., extracting isolated single-neuron activity from extracellular signals). In this work, we used synthetic ground-truth recordings with controlled levels of correlations among neurons to quantitatively benchmark the performance of state-of-the-art spike sorters focusing specifically on spike collisions. Our results show that while modern template-matching-based algorithms are more accurate than density-based approaches, all methods, to some extent, failed to detect synchronous spike events of neurons with similar extracellular signals. Interestingly, the performance of the sorters is not largely affected by the spiking activity in the recordings, with respect to average firing rates and spike-train correlation levels. Since the performances of all modern spike sorting algorithms can be affected as function of the activity of the recorded neurons, scientific claims on correlations and synchrony should be carefully assessed based on the analysis provided in this paper.

**Key words:** benchmark; overlapping spikes; spike collision; spike sorting

## Significance Statement

High-density extracellular recordings allow experimentalists to get access to the spiking activity of large neuronal population, via the procedure of spike sorting. It is widely known that spike sorters are affected by spike collisions, i.e., the occurrence of spatiotemporally overlapping events, but a quantitative benchmark is still lacking. In this contribution, we perform systematic comparisons on the performance of many different spike sorters against spike collisions, showing that modern spike sorters, to different degrees, are still affected by synchronous events. Our results suggest that scientific claims on neuron correlations and synchrony should be carefully assessed as they could result from spike sorting errors.

## Introduction

Assessing the activity of large ensemble of neurons is a crucial challenge in neuroscience. In recent years, multi-electrode arrays (MEAs) and large silicon probes have been developed to record simultaneously from hundreds of electrodes packed with a high spatial density, both *in vivo* (Jun et al., 2017; Angotzi et al., 2019) and *in vitro*

(Berdondini et al., 2009; Frey et al., 2009). With these devices, each electrode records the extracellular field in its vicinity and can detect the action potentials (or spikes) emitted by the neighboring neurons in the tissue. In contrast to intracellular recording, extracellular recordings do not give a direct and unambiguous access to single

Received March 11, 2022; accepted June 23, 2022; First published September 28, 2022.

The authors declare no competing financial interests.

Author contributions: S.G., A.P.B., and P.Y. designed research; S.G., A.P.B., and P.Y. performed research; S.G., A.P.B., and P.Y. contributed unpublished reagents/analytic tools; S.G., A.P.B., and P.Y. analyzed data; S.G., A.P.B., and P.Y. wrote the paper.

neuron activity and one needs to further process the recorded signals to extract the spikes emitted by the different cells around the electrodes. This complex problem of source separation is termed “spike sorting.” While various solutions for small number of channels (tens at max) can be found in the large literature on spike sorting algorithms (Quiroga et al., 2004), these new devices with thousands of channels challenge the classical approach to perform spike sorting.

Recently, a new generation of spike sorting algorithms have been developed to be able to deal with hundreds (or even thousands) of channels recorded simultaneously (for recent review, see Lefebvre et al., 2016; Hennig et al., 2019). The extent to which these modern spike sorting algorithms recover all the spikes from a neuronal population is still under investigations, and might differ depending on the species, tissue, cell types, activity level. While most of the real ground truth recordings (Neto et al., 2016; Yger et al., 2018) are assessing the performance at the single cell level, to obtain an exhaustive assessment of the spike sorting performance at the population level, one must turn to use fully artificial or hybrid dataset (Buccino and Einevoll, 2020; Magland et al., 2020) to properly compare and quantify the performances of the algorithms. But even with such dataset, in most of the studies, errors are only measured as false positive (FP)/false negative (FN) rates, and the reasons behind failures of the algorithms are often overlooked.

In this study, we focused on a key property of the spike trains, at the core of most of these failures, i.e., their fine temporal correlations. Indeed, temporal correlations are ubiquitous in the brain, and the higher the number of recorded cells because of the increased density of the probes, the more prominent they are. Correlations might have an important role in population coding (for review, see Averbek et al., 2006), but correlated activity for nearby cells results, in the extracellular signals, in overlapping activities and thus are harder to identify than isolated spikes. While pioneering work (Pillow et al., 2013) claimed that template-matching-based algorithms were more suited to recover overlapping spikes (either in space and/or time), the extent to which they are is not properly defined. In this work, our aim is to estimate how good (or bad) modern spike sorters are in recovering colliding spikes. What are the limits of the sorters, and what are the key parameters of the recordings and/or of the neurons that could influence these numbers?

This work was supported by the ETH Zurich Postdoctoral Fellowship 19-2 FEL-17 (to A.P.B.)

\*S.G., A.P.B., and P.Y. contributed equally to this work.

Correspondence should be addressed to Samuel Garcia at [samuel.garcia@cnrs.fr](mailto:samuel.garcia@cnrs.fr).

<https://doi.org/10.1523/ENEURO.0105-22.2022>

Copyright © 2022 Garcia et al.

This is an open-access article distributed under the terms of the Creative Commons Attribution 4.0 International license, which permits unrestricted use, distribution and reproduction in any medium provided that the original work is properly attributed.

## Materials and Methods

All the code used to generate the figures is available at <https://spikeinterface.github.io/>.

### Simulated datasets

We used the MEArec simulator (Buccino and Einevoll, 2020) to generate 30-min-long synthetic ground truth recordings. In brief, MEArec uses biophysically detailed multi-compartment models to simulate the extracellular action potentials, or so called “templates.” For this study, we used 13 cell models from layer 5 of a juvenile rat somatosensory cortex (Markram et al., 2015; Ramaswamy et al., 2015) to get a dictionary of biologically plausible templates. Given this database, we took the layout of a NeuroNexus probe (A1x32-Poly3-5 mm-25s-177-CM32 with 32 electrodes in three columns and hexagonal arrangement, a x-pitch and y-pitch of 18 and 22  $\mu\text{m}$ , respectively, and an electrode radius of 7.5  $\mu\text{m}$ ), and randomly positioned 20 cells in the vicinity of the probe, so that every simulated neuron has a unique template (i.e., average extracellular action potential). Templates are then combined with spike trains and slightly modulated in amplitude to add physiological variability. Additive uncorrelated Gaussian noise is finally added to the traces. We generated simulated recordings with 20 neurons randomly positioned in front of the probe, a noise level of 5  $\mu\text{V}$  and a sampling rate of 32 kHz. To obtain more robust results, we generated five recording per conditions with various random seeds. The spike times were kept unchanged, but the positions and the templates of the 20 neurons were changed in each of the individual recording. This allowed us to populate the distribution of cosine similarities between pairs.

### Generating spike trains with controlled correlations

To generate the recordings with various firing rates and correlations levels, we used the mixture process method described in (Brette, 2009). Since by default the method generates controlled cross-correlograms with a decaying exponential profile, we modified it to generate cross-correlograms with a Gaussian profile, to have more synchronous firing for small lags. By setting three different rate levels (5, 10, and 15 Hz) and three different correlation levels (0%, 10%, and 20%) this gave rise to nine conditions, so to 45 recordings in total (five recordings per conditions; see above).

### Template similarity

We define the template for neuron  $i$  as  $\mathbf{T}_i \in \mathbb{R}^{T \times C}$ , with  $T$  representing the number of samples and  $C$  the number of channels. After flattening the template by concatenating the signals from different channels ( $\mathbf{T}_i^f \in \mathbb{R}^{T \cdot C}$ ), the similarity between two neurons  $i$  and  $j$  is quantified via the cosine similarity defined as follows:

$$\text{similarity} = \frac{\mathbf{T}_i^f \cdot \mathbf{T}_j^f}{\|\mathbf{T}_i^f\| \|\mathbf{T}_j^f\|} = \cos(\theta), \quad (1)$$

where  $\theta$  is the angle between the two  $(T \cdot C)$ -dimensional vectors  $\mathbf{T}_i^f$  and  $\mathbf{T}_j^f$ . The cosine similarity is therefore

bounded between  $-1$  (templates are anti-parallel) and  $1$  (templates are parallel). A cosine similarity of  $0$  means that the templates are orthogonal.

### Spike sorters

All the spike sorters used in this study were run using the SpikelInterface framework (Buccino et al., 2020), with default parameters. The following are the exact versions that we used for the different spike sorters: Tridesclous (1.6.4), Spyking-circus (1.0.9; Yger et al., 2018), HerdingSpikes (0.3.7; Hilgen et al., 2017), Kilosort (v1, 2, or 3; Pachitariu et al., 2016), YASS (2.0; Lee et al., 2020), IronClust (5.9.8; Chung et al., 2017), and HDSort (1.0.3; Diggelmann et al., 2018). The desktop machine used has 36 Intel Xeon(R) Gold 5220 CPU @ 2.20 GHz, 200Go of RAM and a Quadro RTX 5000 with 16 Gb of RAM as a GPU.

### Spike sorting comparison

All the quantitative metrics between the results of the spike sorting software and the ground-truth recording were made via the SpikelInterface toolbox.

When comparing a spike sorting output to the ground-truth spiking activity, first an agreement score between each pair of ground-truth and sorted spike trains is computed as:

$$score_{ij} = \frac{\#n_{matches}}{\#n_{igt} + \#n_{sorted} - \#n_{matches}},$$

where  $\#n_{igt}$  and  $\#n_{sorted}$  are the numbers of spikes in the  $i$ -th ground-truth spike train and the  $j$ -th sorted spike trains, respectively.  $\#n_{matches}$  is the number of spikes within  $0.4$  ms between the two spike trains.

Once scores for all pairs are computed, a Hungarian assignment is used to match ground-truth units to sorted units (Buccino et al., 2020). All spikes from matched spike trains are then labeled as: true positive (TP), if the spike is found both in the ground-truth and the sorted spike train; FP, if the spike is found in the sorted spike train, but not in the ground-truth one; and FN, if the spike is only found in the ground-truth spike train.

After labeling all matched spikes, we can now define these unit-wise performance metrics for each ground-truth unit that has been matched to a sorted unit:

$$accuracy = \frac{\#TP}{\#TP + \#FP + \#FN} \quad (2)$$

$$precision = \frac{\#TP}{\#TP + \#FP} \quad (3)$$

$$recall = \frac{\#TP}{\#TP + \#FN} \quad (4)$$

The global accuracy, precision, and recall values shown in Figure 2D are the average values of the performance metrics computed by unit.

Using the unit metrics and the output of the matching procedure, we can further classify each sorted unit as:

Well detected: sorted units with an accuracy  $\geq 0.8$ ;

False Positive: sorted units that are not matched to any ground-truth unit and have a score  $< 0.2$ ;

Redundant: sorted units that are not the best match to a ground-truth unit but have a score  $\geq 0.2$ ;

Overmerged: sorted units with a score  $\geq 0.2$  with more than one ground-truth unit.

In order to generate the spike lag versus recall figures (e.g., Figs. 3-6) we expanded the SpikelInterface software with several novel comparison methods and visualization widgets. In particular, we extended the ground-truth comparison class to the CollisionGTComparison, which computes performance metrics by spike lag. In addition to the agreement score computation and the matching described in the previous paragraphs, this method first detects and flags all “synchronous spike events” in the ground-truth spike trains. Two spikes from two separate units are considered to be a “synchronous spike event” if their spike times occur within a time lag of  $2$  ms. The synchronous events are then binned in  $11$  bins spanning the  $[-2, 2]$  ms interval, and the collision recall is computed for each bin. With a similar principle, we implemented the CorrelogramGTComparison to compute the lag-wise relative errors in cross-correlograms between ground-truth units and spike sorted units.

## Results

### Generation of the ground-truth recordings

To test how robust the recently developed spike sorting pipelines are against spike collisions (Pachitariu et al., 2016; Chung et al., 2017; Hilgen et al., 2017; Yger et al., 2018; Lee et al., 2020), we generated synthetic datasets using the MEArec simulator (Buccino and Einevoll, 2020; see Materials and Methods). More precisely, we took the layout of a NeuroNexus probe with 32 electrodes in three columns and hexagonal arrangement, and randomly positioned 20 cells in the vicinity of the probe (see Fig. 1A), so that every simulated neuron has a unique template (i.e., average extracellular action potential). Figure 1B shows three sample templates with, respectively, low, almost null, and high similarity. The similarity between templates is computed as the cosine similarity of the flattened signals (see Materials and Methods) and the random generation of the positions and cell types of the simulated neurons (and thus of the templates) gives rise to the similarity matrix displayed in see Figure 1C. This similarity, as expected, decreases with the distance between the neurons, computed either from the ground-truth positions of the cells from the simulation or estimated as the barycenters of the templates (Fig. 1D). The more negative the similarity is, the more templates are “in opposition”; the more positive it is, the more templates are “similar.” A similarity close to  $0$  means that templates do not overlap and are strongly orthogonal, i.e., dissimilar. Importantly, the simulations allowed us to cover rather uniformly the space of cosine similarities between templates, which will be used to assess the performance of spike sorters during collisions (Fig. 1E).

To generate the spike trains, we first used a simple approach that forced all the neurons to fire as independent

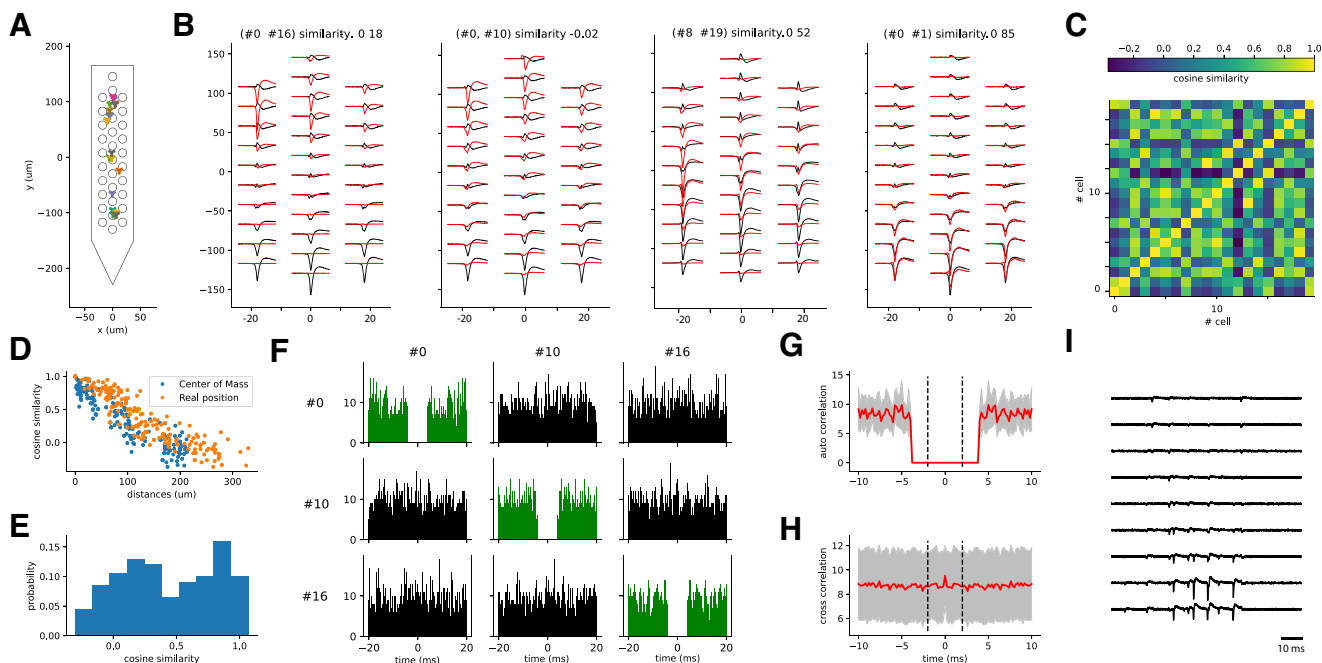


**Figure 1.** Generation of the synthetic recordings. **A**, A total of 20 cells are randomly placed in front of a 32-channel NeuroNexus probe layout. The plot shows the location of each cell for one recording. **B**, Sample template pairs generated by neurons with different cosine similarity values. **C**, Cosine similarity matrix between all pairs of templates for a sample recording. **D**, Cosine similarity as function of the distance between the neurons, either using the real position from the simulations (orange circles), or the estimated barycenter of the templates (blue circles). **E**, Histogram of the cosine similarity distribution from one of the simulated recordings. **F**, Cross-correlograms and auto-correlograms for three sample spike trains. **G**, Average auto-correlograms of all units (red line, gray area represents the SD). **H**, Average cross-correlogram over all pairs of neurons (red line, gray area represents the SD around the mean). **I**, Sample traces from 10 channels of one synthetic recording.

Poisson sources at a fixed and homogeneous firing rate of 5 Hz. To make the simulation more biologically plausible, we pruned all spikes breaking a refractory period violation of 4 ms. The resulting auto-correlograms and cross-correlograms for three sample units are shown in [Figure 1F](#) (auto-correlograms are in green on the diagonal), while [Figure 1G,H](#) display the average (red line) and standard deviation (SD) (gray shaded area) auto-correlation and cross-correlation among all units, respectively. A sample snippet of the generated traces from one recording is shown in [Figure 1I](#), for a subset of 10 channels out of 32. Because of the independence of the Poisson sources, both the average cross-correlograms ([Fig. 1G](#)) and auto-correlograms, outside the  $\pm 4$  ms used as refractory period ([Fig. 1H](#)), are flat.

### Global performance of the spike sorters

In order to assess the global performances of the sorting procedure on our synthetic datasets, we generated five recordings with various random seeds and averaged the results. [Figure 2](#) summarizes the main findings. First, we noticed that, as seen in [Figure 2A](#), the run time was roughly constant across sorters, except for HDSort, with its higher run time. The number of well detected units is similar among sorters, as shown in [Figure 2B](#), but it is worthwhile noticing that Kilosort 3 is the only sorter producing many FP and redundant units (see Materials and Methods for classification of units). Kilosort 2 and HDSort

also identify more FP than well detected units. Importantly, we did not perform any curation of the spike sorting output, but we consider the raw output of each sorter as is.

To check whether all sorters correctly discovered all templates, we computed the cosine similarity between the ground-truth templates from the simulations and the ones found by the sorters, comparing such a metric with the accuracy. By doing so, we wanted to rule out the fact that the sources of the errors could primarily be because of problems in the clustering. Indeed, if the spike sorting algorithms are properly behaving, they should find templates very similar to the ground-truth ones. As it can be seen in [Figure 2C](#), all sorters are on average finding the correct templates, with the notable exception of YASS (in gray) and to some less extent HDSort (in red). The average cosine similarity between found and ground-truth templates is larger than 0.97 for most template-matching-based sorters (Spyking-circus, Kilosort 1/2/3, IronClust, Tridesclous), so we can safely assume that most of the errors are not because of the clustering step. Moreover, the overall accuracy of most of the spike sorters is relatively high ( $\sim 0.95$ ), except for HDSort and HerdingSpikes which yield lower scores ([Fig. 2D](#)). However, this averaged number does not tell us anything regarding the nature of these errors. While this error rate might seem low, it is likely that it is crucial, since it can potentially originate from the collisions, and thus from the correlations among neurons.



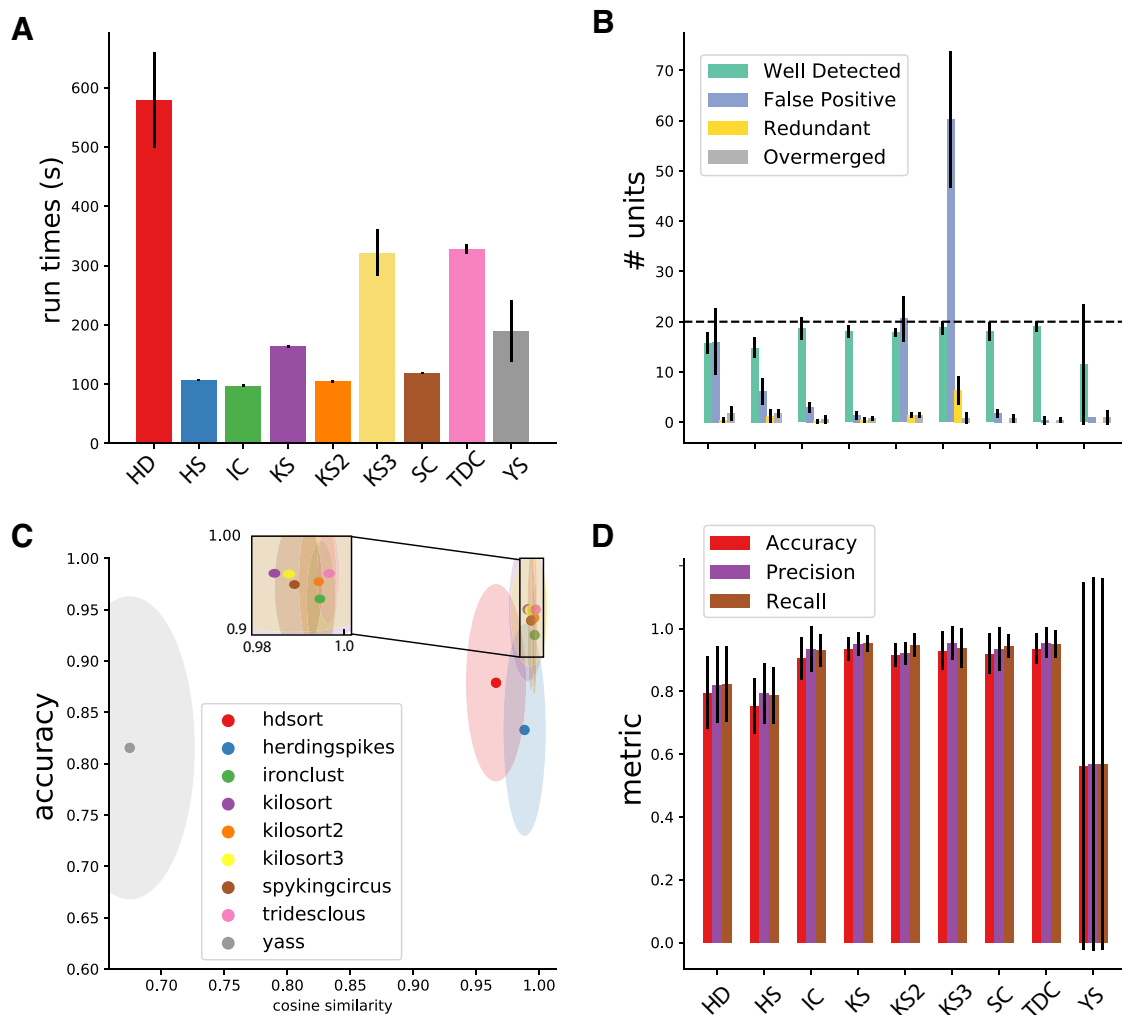


**Figure 2.** Spike sorting performance. **A**, Average run times over five different recordings (see Materials and Methods) for all the tested sorters. Errors bars indicate the SD over multiple recordings. **B**, Average number of cells found by the sorters that are either well detected, redundant, overmerged, or considered as FP (see Materials and Methods). Error bars indicates SD over multiple recordings. **C**, The average cosine similarity between templates found by the sorters and ground-truth templates, as function of the accuracy for the given neurons. Ellipses shows standard error of the means in cosine similarity (x-axis) and accuracy (y-axis). **D**, Average metrics (accuracy, precision, recall; see Materials and Methods) for all the sorters. Error bars show SD over multiple recordings.

**Spike sorting performance is affected by spike collisions**

Using fully synthetic recordings with exhaustive ground truth, we can look at how good individual spike sorters perform specifically with respect to spatiotemporal collisions. To do so, we computed the collision recall (see Materials and Methods) as a function of the lag between two spikes, for a given pair of neurons. By averaging over multiple pairs of ground-truth neurons with similar template similarity (and over multiple recordings; see Materials and Methods), we can obtain a picture of how accurate the sorters are specifically with respect to the spike time lags and the similarities between templates. Figure 3 displays the collision recall per sorter as a function of the lag (x-axis), colored by the similarity between templates. Each panel shows the performance of a different spike sorter. One can immediately see that only few sorters are able to accurately

resolve lag correlations that are close to zero, even when templates are strongly orthogonal (low cosine similarity). This is the case for Kilosort 1 and 2, and for Spyking-circus, all of which use a template-matching procedure that should theoretically explain this behavior. It is worthwhile noting that the decrease in performance for Kilosort 3 is surprising, since the authors confirmed the software is using the exact same template-matching procedure than in previous versions. This means that errors are likely originating either from subtle variations in the preprocessing steps, and/or in the clustering that has been changed and thus might lead to slight differences in the templates. However, while performances are still good for Kilosort 1 and 2 even when the average cosine similarity between pairs is increased, they slightly degrade for Spyking-circus. Density-based sorters (HerdingSpikes and IronClust), on the other hand, do not have a spike collision

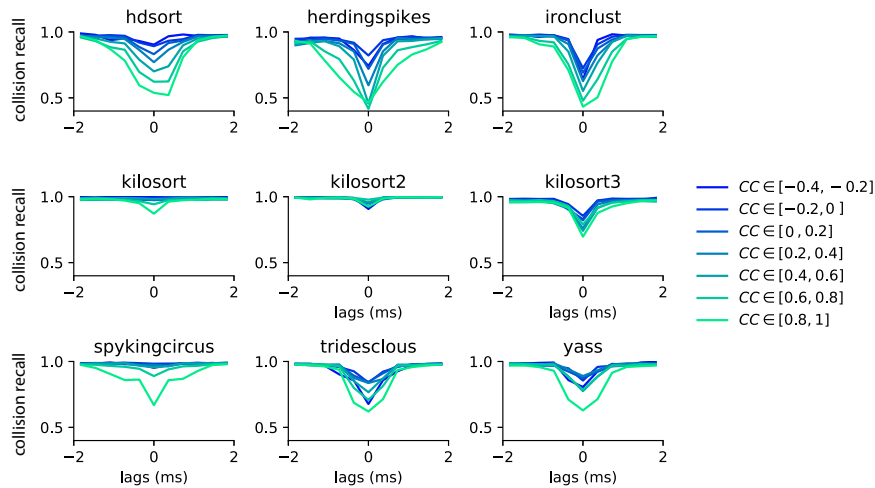


**Figure 3.** Collision recall per sorter. Error (quantified as the collision recall; see Materials and Methods) for various sorters and for all possible lags (between  $-2$  and  $2$  ms), as function of the similarity between the pairs of templates (color code). All curves are averaged over multiple pairs and multiple recordings (see Materials and Methods).

resolution strategy and this is reflected by their overall poorer performance. It is interesting to notice that Tridesclous, HDSort, YASS, and Kilsort 3, also using a template-matching-based procedure to resolve the spikes, are not properly resolving the temporal correlations even for dissimilar templates. Different template-matching strategies are probably the cause of the differences among sorters. For example, HDSort does not implement any strategy for spike collision resolution (Diggelmann et al., 2018), and that is reflected in the quick degradation of performance as template similarity increases. Kilosort uses a GPU-based implementation of the k-SVD algorithm (Aharon et al., 2006), used in matching learning as a dictionary learning algorithm for creating a dictionary for sparse representations. By doing so, it performs a reconstruction of the extracellular traces by optimizing both the templates and the spike times, which is an enhancement compared with what is done in Spyking-circus and Tridesclous. This might explain the boost in performance especially striking for templates with high similarity (similarity  $> 0.8$ ).

#### Generation of controlled spike collision simulated data

The results shown in the previous section have been obtained only in a particular regime of activity, with all neurons firing independently as Poisson sources with an average firing rate of 5 Hz. However, neurons usually do not fire independently of each other, but rather have intrinsic correlations, also depending on different brain areas, brain states, and species. In addition, the average firing rates can also largely vary depending on brain areas. As an example, it is well known that Purkinje cells in the cerebellum have a very high firing rate (Sedaghat-Nejad et al., 2021), that networks tends to synchronize their activity either in slow waves during sleep (Steriade, 2004), or during pathologic activity [such as epileptic seizures (Truccolo et al., 2011)]. Therefore, assessing how performances may

vary during different conditions is important to generalize our observations.

In order to study how spike sorting is affected by correlations and firing rates, we used a mixture procedure (Brette, 2009) that allowed us to control precisely the shape of the auto-correlograms and cross-correlograms for the injected spike trains. More precisely, we decided to explore in a systematic manner three rate levels (5, 10, and 15 Hz), and three correlation levels (0%, 10%, and 20%). Note that the 5 Hz firing rate with 0% correlation corresponds to the scenario displayed in Figures 2 and 3.

Figure 4 shows the average of cross-correlograms and auto-correlograms and the spike trains of a recording where cells are firing as independent Poisson sources at 5 Hz in panels A–C (and thus with 0% correlation, as shown by the flat average cross-correlograms in Fig. 4A) and at 15 Hz with 20% correlation (Fig. 4D–F). Although experimental recordings would contain a broader spectrum of firing rates and correlations, here we focus on assessing how different firing regimes affect spike sorting performance in a controlled setting. By varying these conditions, we wanted to challenge the internal clustering step of the spike sorting algorithms and see how generalizable are the results we observed in the previous section. One would expect that the increased density of spikes (both in terms of firing rates and of synchrony) should degrade the performance of the spike sorters by affecting both the clustering step and the template-matching step, which in turn would degrade the resolution of spike collisions. It is worthwhile noting that all the rates and correlation levels are homogeneous among neurons and only the templates are different.

#### Do correlations and firing rates affect spike sorting of spike collisions?

To assess whether firing rate and spike train correlation affect spike sorting performance, we selected all unit

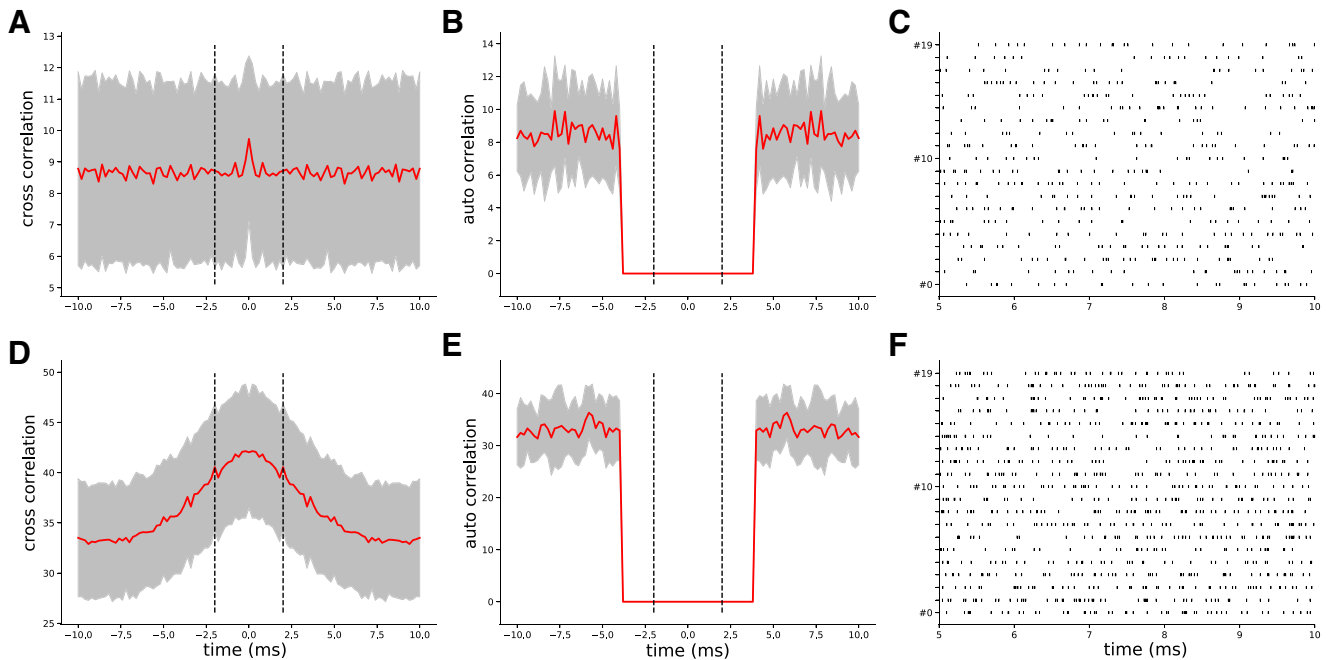


**Figure 4.** Controlling spike trains correlations and firing rates. **A**, Average cross-correlograms between all pairs of distinct neurons firing as independent Poisson sources at 5 Hz (red curve, gray area represents the SD). **B**, Same as **A**, but for auto-correlograms. **C**, Raster plot showing the activity of the uncorrelated neurons firing at 5 Hz. **D-E**, Same as **A-B**, but for a rate of 15 Hz and 20% correlation. **F**, Raster plot showing the activity at 20% correlation and 15 Hz rate.

pairs with a similarity  $>0.5$ . We first averaged the recall curves for all template similarities (i.e., we averaged the curves with similarity  $>0.5$  shown in Fig. 3).

In Figure 5A, we show the recall with respect to the spike lags averaged over all nine configurations (three firing rates  $\times$  three correlations) for each sorter. The thick line represents the mean recall and the shaded area is the SD over different rate-correlation configuration. All sorters, except YASS, appear to have a very consistent curve (low SD) over different configurations and do not seem affected by changes in average firing rates and correlations in the spike trains. YASS' large SD can be explained by looking at individual recall curves at different rate-correlation regimes (Fig. 6, yellow lines): the spike sorting performance degrades with increasing firing rates, but it

does not seem to be strongly affected by increased correlation rates. However, we should stress that since the collision recall is a relative measure, the same value for a larger number of spikes (when firing rate is increased) means that overall, there are more misses for all sorters.

Similar considerations can be done by looking at the average recall with respect to template similarity (Fig. 5B). To construct these plots, we integrated the curves in Figure 3 over lags for different cosine similarities. Also in this case, the curves appear consistent (low SD) with the exception of YASS, for which recall is reduced with increased firing rate regimes (Fig. 7, yellow lines). It is worth noticing that when the cosine similarity becomes negative, all the sorters perform very poorly in properly resolving the overlaps. This could be explained by the fact that when a pair of

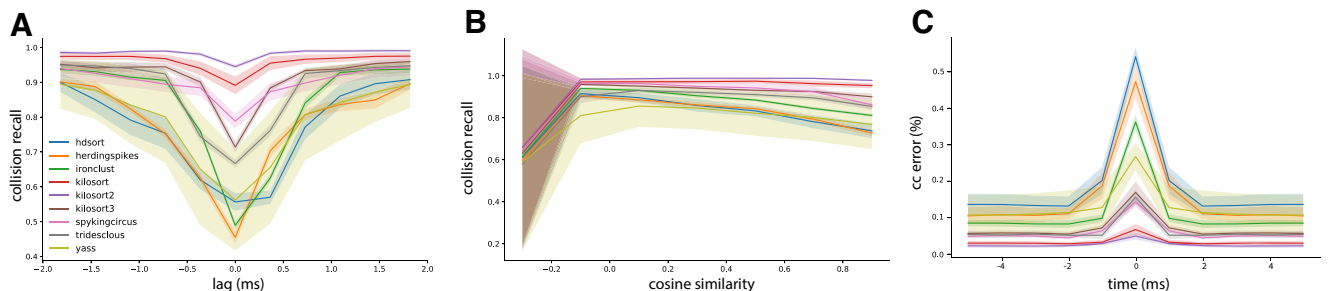


**Figure 5.** Spike sorting performance for different conditions. **A**, Average collision recall over the nine conditions shown in Figure 6 (3 firing rate levels and 3 correlation levels) as function of the lag between spikes, for pairs of cells with cosine similarity higher than 0.5. The shaded area shows the SD over the conditions. **B**, Similarly as **A**, the average collision recall as function of the cosine similarity between pairs of cells. **C**, Mean relative error between the ground-truth cross-correlograms and the estimated ones, for all sorters, averaged over all pairs with a similarity higher than 0.5.

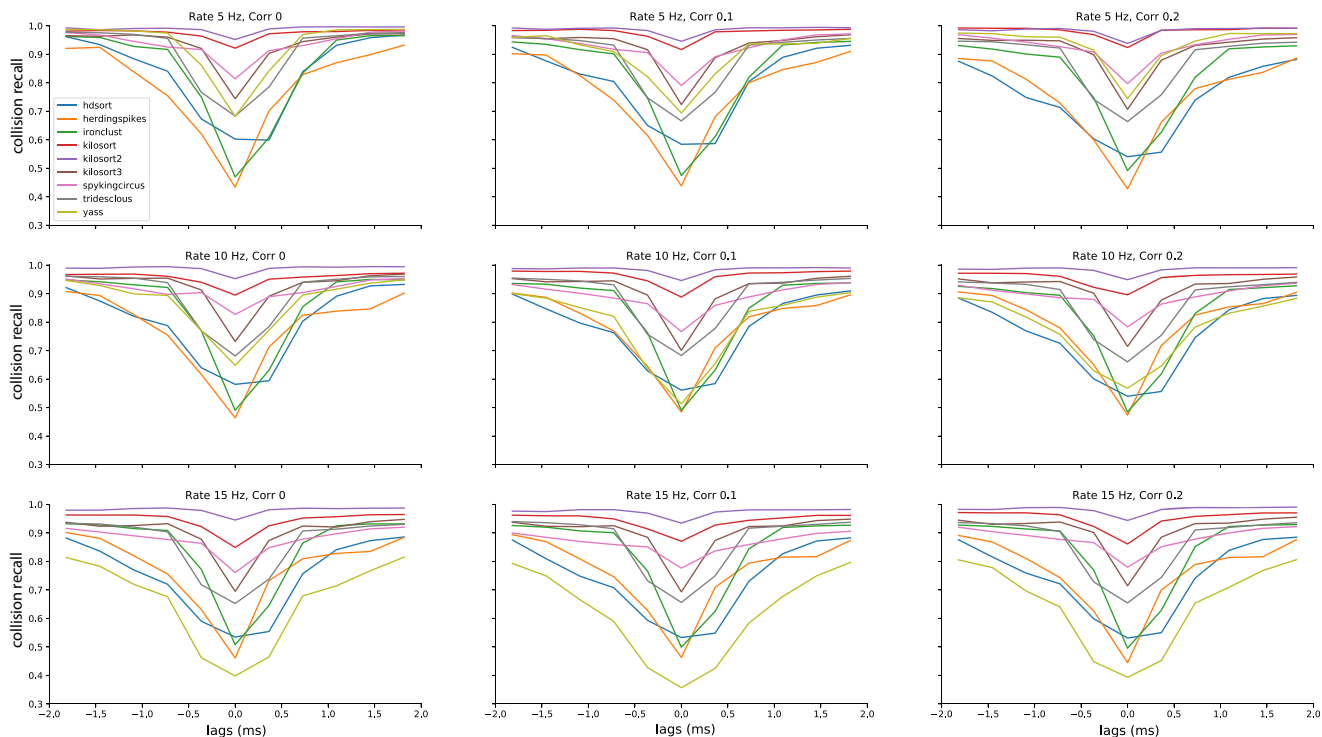


**Figure 6.** Average performances of the spike sorters as function of the temporal lags. Each panel shows the average collision recall for template pairs with a similarity above 0.5 for a different condition, in terms of firing rate and correlation levels.

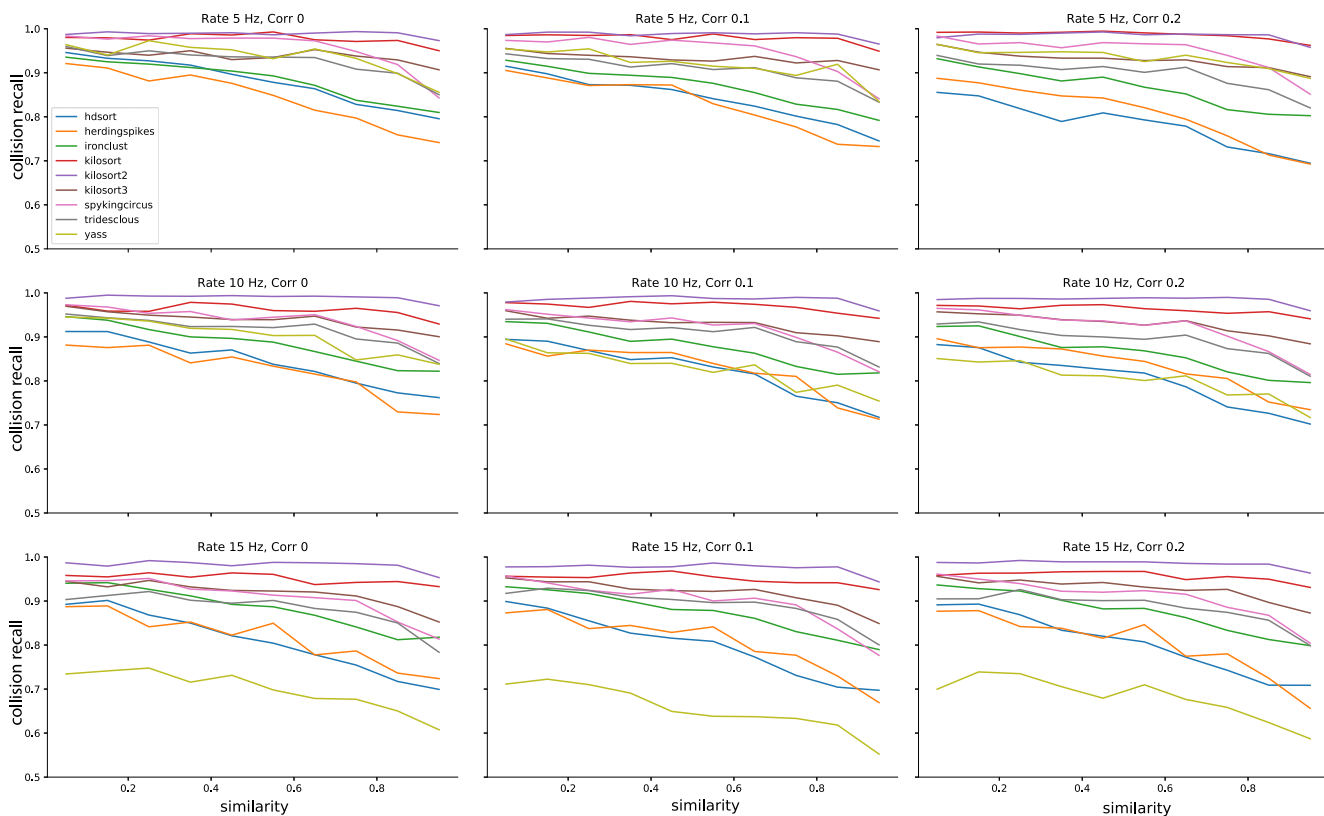


**Figure 7.** Average performances of the spike sorters as function of the template similarity. Each panel shows the average collision recall over all lags in  $[-2, 2]$  ms for a different condition, in terms of firing rate and correlation levels.



templates is anti-parallel (Fig. 1A, left panel), a subset of electrodes might show a negative signal for one template and a positive signal from the other (because of return currents in the dendritic signals; Gold et al., 2009). Effectively, when a spike collision between the two spikes occurs, this would lower the amplitude of the negative peak, which could reduce the detectability of the spike.

The collision recall metric is mostly useful to obtain a quantitative insight on the behavior of the spike sorting algorithms, but how do these errors transpose in practical situations? To assess this, we measure the relative error (in percentage) between the ground-truth cross-correlograms and the ones computed from the spike sorting outputs. We then averaged these error curves among all recordings and experimental conditions (firing rates and synchrony levels). As shown in Figure 5, the error in the estimated cross-correlogram can be as large as  $>50\%$  for small lags, and for some spike sorting algorithms such as HDSort, HerdingSpikes, or IronClust. Moreover, it is also worth noticing the baseline error rate is not the uniform across sorters. From this metric, we can again conclude that template-matching-based spike sorting algorithms such as Kilosort (1, 2, and 3), Spyking-circus, or Tridesclous are much better to resolve fine temporal correlations among neurons.

## Discussion

In this study, we showed in a systematic and quantitative manner how spatiotemporal correlations can be underestimated during spike sorting. Using synthetic datasets, we compared a large diversity of modern spike sorters and showed how they behaved as function of the similarity between the templates and the temporal lags between spikes. As expected, the closer the spikes are in time, the harder is it, for all sorter, to properly resolve the overlaps. However, more interestingly, the more similar the templates are, the higher the failures are. These failures are striking especially for spike sorters that are not relying on template-matching-based approaches (HerdingSpikes, IronClust). For the ones using a template-matching-based approach (Kilosort, Spyking-circus, Tridesclous, HDSort), the problem is less pronounced (with the exception of HDSort) but still present, and therefore this phenomenon should be taken into account when making claims about the synchrony.

To our surprise, the global behavior of the spike sorters did not depend much on the overall firing rate and/or the correlation levels. This allows us to generalize the findings and we think that the quantitative results shown here could be translated to various *in vitro* or *in vivo* recordings from different brain regions and species. As shown in Figure 5, while the variability over different conditions is rather high for some algorithms, template-matching-based algorithms tend to be rather robust and overall better in resolving spike collisions. This is a very encouraging sign toward a unified and reproducible automated solution for spike sorting (Buccino et al., 2020; Magland et al., 2020), agnostic of the recording conditions.

The results shown in the paper were obtained with purely artificial recordings, since we need exhaustive

information on the ground-truth spiking activity of all neurons to quantitatively compare and benchmark different spike sorters. However, it would be interesting to generalize these observations with real recordings, assuming one would have a proper ground truth at the population level. Indeed, such a ground truth is needed to compute the collision recall and see how sorters behave as function of lags and similarities between templates. To our knowledge, such a ground truth does not exist (Neto et al., 2016; Diggelmann et al., 2018; Yger et al., 2018). While one could try to generate an “approximated” ground truth by combining the output of several spike sorters with an ensemble spike sorting approach (as in Buccino et al., 2020), the disagreements among sorters are currently so high that this process is hard if not impossible, if one wants to sample from a large number of pairs.

While missing spikes for very dissimilar templates and small lags is problematic, the errors made for very similar templates may be less frequent depending on the probe layout and neuronal preparation. Indeed, such errors strongly depend on the distribution of template similarities between all pairs of recorded cells, and this distribution might differ from recording to recording. For example, in the retina (Wässle, 2004) one would expect highly synchronous cells, of the same functional type, to be far apart from each other because of an intrinsic tiling of the visual space. Such properties are unknown *in vivo* or in cortical structures, but might bias the distribution of template similarities between nearby neurons, and thus modify the estimation of collision recalls.

## References

- Aharon M, Elad M, Bruckstein A (2006) K-SVD: an algorithm for designing overcomplete dictionaries for sparse representation. *IEEE Trans Signal Process* 54:4311–4322.
- Angotzi GN, Boi F, Lecomte A, Miele E, Malerba M, Zucca S, Casile A, Berdondini L (2019) Sinaps: an implantable active pixel sensor cmos-probe for simultaneous large-scale neural recordings. *Biosens Bioelectron* 126:355–364.
- Averbeck BB, Latham PE, Pouget A (2006) Neural correlations, population coding and computation. *Nat Rev Neurosci* 7:358–366.
- Berdondini L, Imfeld K, Maccione A, Tedesco M, Neukom S, Koudelka-Hep M, Martinoia S (2009) Active pixel sensor array for high spatio-temporal resolution electrophysiological recordings from single cell to large scale neuronal networks. *Lab Chip* 9:2644–2651.
- Brette R (2009) Generation of correlated spike trains. *Neural Comput* 21:188–215.
- Buccino AP, Einevoll GT (2020) Mearec: a fast and customizable testbench simulator for ground-truth extracellular spiking activity. *Neuroinformatics* 19:185–204.
- Buccino AP, Hurwitz CL, Garcia S, Magland J, Siegle JH, Hurwitz R, Hennig MH (2020) Spikeinterface, a unified framework for spike sorting. *Elife* 9:e61834.
- Chung JE, Magland JF, Barnett AH, Tolosa VM, Tooker AC, Lee KY, Shah KG, Felix SH, Frank LM, Greengard LF (2017) A fully automated approach to spike sorting. *Neuron* 95:1381–1394.
- Diggelmann R, Fiscella M, Hierlemann A, Franke F (2018) Automatic spike sorting for high-density microelectrode arrays. *J Neurophysiol* 120:3155–3171.
- Frey U, Egert U, Heer F, Hafizovic S, Hierlemann A (2009) Microelectronic system for high-resolution mapping of extracellular

- electric fields applied to brain slices. *Biosens Bioelectron* 24:2191–2198.
- Gold C, Girardin CC, Martin KA, Koch C (2009) High-amplitude positive spikes recorded extracellularly in cat visual cortex. *J Neurophysiol* 102:3340–3351.
- Hennig MH, Hurwitz C, Sorbaro M (2019) Scaling spike detection and sorting for next-generation electrophysiology. *Adv Neurobiol* 22:171–184.
- Hilgen G, Sorbaro M, Pirmoradian S, Muthmann JO, Kepiro IE, Ullo S, Ramirez CJ, Puente Encinas A, Maccione A, Berdondini L, Murino V, Sona D, Cella Zancacchi F, Sernagor E, Hennig MH (2017) Unsupervised spike sorting for large-scale, high-density multielectrode arrays. *Cell Rep* 18:2521–2532.
- Jun JJ, et al. (2017) Fully integrated silicon probes for high-density recording of neural activity. *Nature* 551:232–236.
- Lee J, Mitelut C, Shokri H, Kinsella I, Dethe N, Wu S, Li K, Reyes EB, Turcu D, Batty E, Kim YJ, Brackbill N, Kling A, Goetz G, Chichilnisky EJ, Carlson D, Paninski L (2020) YASS: yet another spike sorter applied to large-scale multi-electrode array recordings in primate retina. *bioRxiv*. doi:10.1101/2020.03.18.997924.
- Lefebvre B, Yger P, Marre O (2016) Recent progress in multi-electrode spike sorting methods. *J Physiol Paris* 110:327–335.
- Magland J, Jun JJ, Lovero E, Morley AJ, Hurwitz CL, Buccino AP, Garcia S, Barnett AH (2020) Spikeforest, reproducible web-facing ground-truth validation of automated neural spike sorters. *Elife* 9:e55167.
- Markram H, et al. (2015) Reconstruction and simulation of neocortical microcircuitry. *Cell* 163:456–492.
- Neto JP, Lopes G, Frazão J, Nogueira J, Lacerda P, Baião P, Aarts A, Andrei A, Musa S, Fortunato E, Barquinha P, Kampff AR (2016) Validating silicon polytrodes with paired juxtacellular recordings: method and dataset. *J Neurophysiol* 116:892–903.
- Pachitariu M, Steinmetz NA, Kadir SN, Carandini M, Harris KD (2016) Fast and accurate spike sorting of high-channel count probes with kilosort. *NIPS* 2016:4448–4456.
- Pillow JW, Shlens J, Chichilnisky EJ, Simoncelli EP (2013) A model-based spike sorting algorithm for removing correlation artifacts in multi-neuron recordings. *PLoS One* 8:e62123.
- Quiroga RQ, Nadasdy Z, Ben-Shaul Y (2004) Unsupervised spike detection and sorting with wavelets and superparamagnetic clustering. *Neural Comput* 16:1661–1687.
- Ramaswamy S, et al. (2015) The neocortical microcircuit collaboration portal: a resource for rat somatosensory cortex. *Front Neural Circuits* 9:44.
- Sedaghat-Nejad E, Fakharian MA, Pi J, Hage P, Kojima Y, Soetedjo R, Ohmae S, Medina JF, Shadmehr R (2021) P-sort: an open-source software for cerebellar neurophysiology. *J Neurophysiol* 126:1055–1075.
- Steriade M (2004) Slow-wave sleep: serotonin, neuronal plasticity, and seizures. *Arch Ital Biol* 142:359–367.
- Truccolo W, Donoghue JA, Hochberg LR, Eskandar EN, Madsen JR, Anderson WS, Brown EN, Halgren E, Cash SS (2011) Single-neuron dynamics in human focal epilepsy. *Nat Neurosci* 14:635–641.
- Wässle H (2004) Parallel processing in the mammalian retina. *Nat Rev Neurosci* 5:747–757.
- Yger P, Spampinato GL, Esposito E, Lefebvre B, Deny S, Gardella C, Stimberg M, Jetter F, Zeck G, Picaud S, Duebel J, Marre O (2018) A spike sorting toolbox for up to thousands of electrodes validated with ground truth recordings in vitro and in vivo. *Elife* 7:e34518.